JOURNAL OF Materials CHEMISTRY

Ruthenium(II) thiocyanate complexes containing 4′-(4-phosphonatophenyl)-2,2′:6′,2″-terpyridine: synthesis, photophysics and photosensitization to nanocrystalline TiO_2 electrodes

Bingwen Jing,[a] Hong Zhang,[b] Manhua Zhang,[a] Zhuhong Lu[b] and Tao Shen[a]

[a]*Institute of Photographic Chemistry, Chinese Academy of Sciences, Beijing 100101, China*
[b]*National Laboratory of Molecular and Biomolecular Electronics, Southeast University, Nanjing 210096, P.R. China*

Several polypyridyl ruthenium(II) complexes [Ru^{II}(ttp-PO_3H)(LL)(NCS)], where ttp-PO_3H = 4′-(4-phosphonatophenyl)-2,2′:6′,2″-terpyridine and LL = 4,4′-dimethyl-2,2′-bipyridine (dmpy), 1,10-phenanthroline (phen) or 2,2′-biquinoline (biquin), were synthesized and characterized. The three structurally analogous complexes show different sensitization to nanocrystalline TiO_2 film electrodes with increasing activity in the sequence LL = biquin, phen, dmpy, the biquin derivative showing almost no sensitization. Investigations demonstrate that the localization of the excited electron of the complexes affects the electron injection efficiency. Results indicate that the excited electron should be localized on the ligand with adsorbent groups attaching to the electrode in the design of complex sensitizers. Evidence of the localization of the excited electron in the ruthenium polypyridine complexes is proposed.

The search for efficient solar energy conversion devices continues to be an important area of research.[1–3] Recently, an attractive approach has been to utilize wide-bandgap oxide semiconductors in photoelectrochemical cells.[4] The extraordinary thermal and photochemical stability of wide-bandgap oxide semiconductors lends them to extensive application for light conversion, but a potential drawback with these materials is their large bandgap which requires high energy light to create electron–hole pairs. The problem has largely been solved by sensitizing them to visible light with dyes. Unfortunately, the light-to-electricity conversion efficiency of conventional dye-sensitized solar cells was very low (<1%) previously, largely because of their low light harvesting efficiency with only one layer of absorbent dye or low charge separation and transfer efficiency with thick dye layers on a flat surface electrode.[5–7] Recently several improvements have substantially raised the light-to-electricity conversion efficiency of dye-sensitized solar cells:[8–26] (1) high-surface-area nanocrystalline porous film electrodes instead of flat electrodes have been used in order to increase incident light harvesting efficiency through more dye being attached on electrode, which overcomes the poor light harvesting efficiency with one layer dye adsorption on a flat electrode and low charge injection with thick dye. (2) Improvement of adsorption performance between dye and electrode using a dye containing strong adsorbent groups which make the dye bind strongly onto the electrode surface, which overcomes the disadvantage of short excited state lifetime of the dye and makes charge injection more efficient. (3) Design and synthesis of more efficient sensitizers. Extensive investigations have shown that porphyrins and complexes of second- and third-row transition metals with polypyridyl ligands possess remarkable sensitization; ruthenium polypyridine complexes, in particular, have proven to be the most efficient sensitizers. Gratzel and coworkers in particular have pioneered this field.[8–18] They obtained >10% light-to-electricity conversion efficiency and up to 17 mA cm^{-2} photocurrent intensity, mainly using nanocrystalline TiO_2 film electrodes and polypyridyl ruthenium sensitizers with ideal spectral characteristics.[15] These results make the practical application of photoelectrochemical cells feasible.[15,22] In order to further improve sensitization of dyes and conversion efficiency of solar cells to acquire practical application, many researchers have studied extensively methods of preparation of electrodes,[27,28] the bonding mode of the dye to the surface of electrode,[29] and design and synthesis of sensitizers[18,29] as well as the micromechanism of energy migration and electron transfer between the sensitizer and the nanocrystalline porous film electrode.[30,31] As is well known, the ligands are one of the main factors affecting the properties of a complex and to study the electron transfer efficiency with different ligands, we have synthesized three new polypyridyl ruthenium sensitizers (**1**–**3**) containing phosphonate groups as adsorbent groups (Scheme 1) and investigated their photophysical properties and their sensitization to TiO_2 nanocrystalline film electrodes.

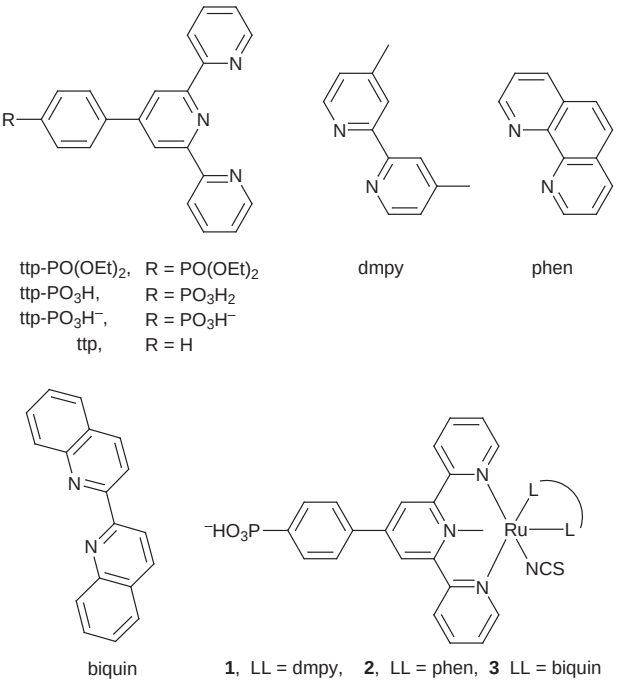

Scheme 1 Structures of ligands used in here and complexes **1**, **2**, **3**

Experimental

Chemicals

4,4′-Dimethyl-2,2′-bipyridine (dmpy), 1,10-phenanthroline (phen), 2,2′-biquinoline (biquin, Merck) and $RuCl_3 \cdot xH_2O$ (Aldrich) were commercial samples and were used without purification. 4′-(*p*-Diethylphosphonatophenyl)-2,2′:6′,2″-terpyridine [ttp-$PO(OEt)_2$] was synthesized according to the literature procedure.[32] Purified solvents were used for electrochemical and spectroscopic measurements.

Syntheses

[Ru{ttp-$PO(OEt)_2$}Cl_3]. 890 mg (2 mmol) ttp-$PO(OEt)_2$, 520 mg $RuCl_3 \cdot 3H_2O$ and 150 ml anhydrous ethanol were refluxed for 4 h and then cooled to room temperature and the precipitate filtered off and washed with anhydrous ethanol and diethyl ether and dried to give 1.178 g of solid product. Yield: 90.2%, Anal. Calc. for [Ru{ttp-$PO(OEt)_2$}Cl_3]: C,46.05; H,3.71; N,6.44. Found: C,46.54; H,3.52; N, 6.93%.

[Ru{ttp-$PO(OEt)_2$}(dmpy)Cl]Cl. 326 mg (0.5 mmol) [Ru{ttp-$PO(OEt)_2$}Cl_3], 96 mg (0.52 mmol) dmpy, 0.8 ml NEt_3 and 100 mg LiCl, were added to 50 ml of ethanol–water (3:1, v/v). The mixture was refluxed with stirring under N_2 for 4 h and a purple solution was obtained. This was then concentrated to dryness by rotary evaporation and purified using a short silica chromatography column with ethanol as eluent. The first eluted purple band was concentrated to give 356 mg of a purple solid. Yield: 87%; Anal. calc. for [Ru{ttp-$PO(OEt)_2$}(dmpy)Cl]Cl·H_2O: C,54.27; H,4.68; N,8.55. Found: C,51.85; H,4.34; N,8.31%.

[Ru(ttp-PO_3H_2)(dmpy)Cl]Cl. 50 ml 6 M HCl aqueous solution of 300 mg [Ru{ttp-$PO(OEt)_2$}(dmpy)Cl]Cl were refluxed under N_2 for 8 h, resulting in a dark red precipitate. The cooled solution was filtered and the precipitate washed with water and diethyl ether to give 248 mg of a dark red solid. Yield: 84.8%, Anal. Calc. for [Ru(ttp-PO_3H_2)(dmpy)Cl]Cl·$3H_2O$: C,49.62; H,4.29; N,8.77. Found: C,49.15; H,3.85; N,8.24%.

[Ru(ttp-PO_3H)(dmpy)(NCS)] 1. 200 mg(0.25 mmol) [Ru(ttp-PO_3H_2)(dmpy)Cl]Cl·$3H_2O$ and 81 mg(1 mmol) NaNCS were added to 30 ml of a methanol–NaOH aqueous solution (pH = 10) and refluxed under N_2 for 4 h. Complex **1** was isolated as a neutral complex at its isoelectric point by acidification with dilute aqueous HCl. The resulting purple solid was washed with cold water, acetone and diethyl ether, to give 110 mg of **1**, Yield: 54.8%, Anal. Calc. for [Ru(ttp-PO_3H)(dmpy)(NCS)]·$4H_2O$: C,50.86; H,4.39; N,10.47. Found: C,51.23; H,4.12; N,10.78%. IR: $\nu_{NCS} = 2094\ cm^{-1}$.

The remainder of the complexes were prepared by analogous methods to that for **1**.

[Ru{ttp-$PO(OEt)_2$}(phen)Cl]Cl. 326 mg (0.5 mmol) [Ru{ttp-$PO(OEt)_2$}Cl_3], 101 mg (0.51 mmol) phen·H_2O, gave 305 mg of product. Yield: 75%, Anal. Calc. for [Ru{ttp-$PO(OEt)_2$}(phen)Cl]Cl. H_2O: C,54.54; H,4.21; N,8.60. Found: C,55.12; H,4.06; N,8.55%.

[Ru(ttp-PO_3H_2)(phen)Cl]Cl. 250 mg(0.3068 mmol) [Ru{tpp-$PO(OEt)_2$)(phen)Cl]Cl·H_2O, gave 202 mg product. Yield: 83% Anal. Calc. for [Ru(ttp-PO_3H_2)(phen)Cl]Cl·$3H_2O$: C,49.88; H,3.81; N,8.81. Found: C,50.12; H,3.56; N,8.64%.

[Ru(ttp-PO_3H)(phen)(NCS)] 2. 150 mg(0.1887 mmol) [Ru(ttp-PO_3H_2)(phen)Cl]Cl·$3H_2O$, 61 mg (0.75 mmol) NaNCS, gave 100 mg of **2**, Yield: 68%, Anal. Calc. for [Ru(ttp-PO_3H)(phen)(NCS)]·$3H_2O$: C,52.30; H,3.74; N,10.76. Found: C,51.77; H,3.58; N,10.28%. IR: $\nu_{NCS} = 2098\ cm^{-1}$.

[Ru{ttp-$PO(OEt)_2$}(biquin)Cl]Cl. 326 mg(0.5 mmol) [Ru{ttp-$PO(OEt)_2$}Cl_3], 131 mg(0.511 mmol) biquin, gave 310 mg product, Yield: 71% Anal. Calc. for [Ru{ttp-$PO(OEt)_2$}(biquin)Cl]Cl: C,59.17; H,4.16; N,8.02. Found: C,58.98; H,4.11; N,8.35%.

[Ru(ttp-PO_3H_2)(biquin)Cl]Cl. 250 mg(0.2864 mmol) [Ru{ttp-$PO(OEt)_2$}(biquin)Cl]Cl gave 193 mg of product, Yield: 79% Anal. Calc. for [Ru(ttp-PO_3H_2)(biquin)Cl]Cl·$2H_2O$: C,54.93; H,3.78; N,8.21. Found: C,55.21; H,3.52; N,7.98%.

[Ru(ttp-PO_3H)(biquin)(NCS)] 3. 150 mg(0.176 mmol) [Ru(ttp-PO_3H_2)(biquin)Cl]Cl·$2H_2O$ and 57 mg(0.7 mmol) NaNCS gave 94 mg of **3**, Yield: 65%, Anal. Calc. for [Ru(ttp-PO_3H)(biquin)(NCS)]·H_2O: C,58.46; H,3.56; N,10.23. Found: C,58.17; H,3.13; N,10.78%. IR: $\nu_{NCS} = 2095\ cm^{-1}$.

Electrode preparation

Transparent TiO_2 films were prepared from commercial TiO_2 powder (Degussa, P25) in a manner analogous to that previously described:[15,23] 6 g TiO_2 powder were ground in a marble mortar with 2 ml water containing 0.2 ml acetylacetone to prevent reaggregation of the particles. After the powder had been dispersed by a high shear force in the viscous paste, it was diluted by slow addition of water (8 ml) under continued grinding. Finally, 0.1 ml Triton-100 detergent was added to facilitate the spreading of the colloid on the substrate. A 3×6 cm plate $30\ \Omega\ \square^{-1}$ conducting glass was used as the substrate for the deposition of the TiO_2. The plate was scribed down the middle and at 1 cm intervals along its length (6 cm). A cellophane tape of 0.5 cm width was glued on each edge of its two long sides. The tapes serve to determine the thickness of the TiO_2 layer as well as to mask an area of the electrode for ohmic contact to the conductive glass. Several drops of TiO_2 solution were distributed on the plate surface and spread uniformly by rolling a 1 cm diameter test tube across the substrate surface, and allowed to air dry. The substrate coated TiO_2 then was heated in a furnace in which the temperature was increased gradually to 500 °C and then kept at 500 °C for 30 min. After this, the substrate was broken into 1.5×1 cm pieces and 1 cm^2 active surface area TiO_2 films were obtained.

Surface attachment of complexes

The complexes were attached to the TiO_2 surface by immersing the processed electrode in *ca.* 10^{-4} M ethanol solutions of the complexes for 24 h. During this time the surface of the electrode changed from white to the color of the attached dye. The electrodes were then removed, thoroughly rinsed in ethanol and stored in air until use in photoelectrochmical experiments. Surface coverages were determined by spectroscopic measurement of the amount of complex in the *ca.* 10^{-4} M ethanol solution before and after the attachment process, or by desorbing the complexes with 2 M NaOH solution.

Electrochemistry

Cyclic voltammograms were recorded on an M270C electrochemical system (EG & G Corp.). Measurements were made at a sweep rate of $100\ mV\ s^{-1}$. The adopted three-electrode system also contained a Pt disc working electrode and a saturated calomel reference electrode. The supporting electrolyte was 0.1 M *n*-tetrabutylammonium perchlorate in DMF. Solutions of samples (*ca.* 5×10^{-4} M) were prepared by dissolution in purified DMF. The solutions were deoxygenated by bubbling with nitrogen for 15 min before each scan. The Pt

working electrode was manually cleaned and polished prior to each individual scan.

Optical measurements

Absorption spectra were recorded using two matched 1 cm glass cells on a Shimadzu UV-1600A recording spectrophotometer. Samples were prepared gravimetrically as *ca.* 3×10^{-5} M ethanol solutions. IR spectra were recorded on KBr pellets with a Perkin Elmer 983G spectrometer. Emission spectra were recorded on a Hitachi 850 fluorescence spectrometer. Emission spectra were collected at maximal absorption in the visible region as excitation wavelength and reported as uncorrected values. Quantum yields were obtained using $[Ru(bpy)_3][PF_6]_2$ in MeCN as a quantum counter calibrant. Emission lifetimes were measured by nanosecond laser flash photolysis using a DCR Nd:YAG laser (532 nm) as the excitation source and SMA (spectrometric multichannel analyzer, Princeton Instruments Inc. OSMA Detector Controller) as detector. The data were then transferred to a 486PC to calculate the lifetimes of the complexes. Samples for emission lifetime and quantum yield measurements were saturated with argon gas for 20 min.

Photoelectrochemistry

Photoelectrochemical measurements were performed in a two-electrode sandwich cell arrangement in which the counter electrode was prepared by sputtering a thin layer of platinum onto the conductive side of a tin dioxide electrode similar in size to the working electrode. The two electrodes were assembled into a 'sandwich' arrangement with 0.3 M LiI and 0.03 M I_2 in propylene carbonate as electrolyte introduced between the two electrodes. The photocurrent and photovoltage were measured with a potentiostat model CMBP-1. Monochromatic illumination was obtained using a 500 W xenon arc lamp in combination with a grating monochromator model WPG3D. The intensity was calibrated using a model FP-3 radiometer-photometer.

Results and Discussion

Photophysical properties

The absorption spectra of complexes **1**–**3** in ethanol solution are shown in Fig. 1. Intense metal-to-ligand charge transfer(MLCT) bands are observed in the visible region and their maximum absorption wavelengths are located at 503, 497 and 572 nm, respectively. Complexes **1** and **2** show room temperature emission in ethanol. The maximum emission wavelengths are 735 nm for **1** and 710 nm for **2**. Complex **3** only exhibits very weak emission under the same conditions. All complexes show pH-dependent absorption spectra in water, with a red shift of their visible absorption maximum upon increasing the pH from 3 to 9. Table 1 also lists the oxidation potentials of the ruthenium complexes, which range from 0.84 to 1.00 V *vs.* SCE. Complex **3** exhibits the highest value, followed by **2** then **1**. This is attributed to π back-bonding, *i.e.*, electron donation from Ru^{II} t_{2g} orbitals to empty π* levels of the ligands, consistent with the π*-accepting ability of biquin > phen > dmpy, which is reflected by their free ligand reduction potentials.

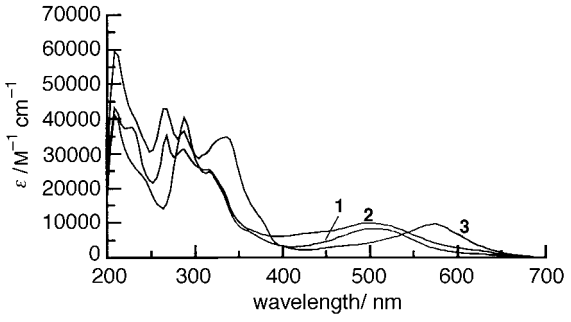

Fig. 1 Absorption of complexes **1**, **2**, **3** in ethanol at room temperature

Fig. 2 shows the absorption spectra of complexes **1**, **2** and **3** adsorbed onto TiO_2 films as well as in ethanol solution. Comparing their absorption in films with in solution, we found that the profiles of the absorption spectra of **1** and **2** in films changed significantly showing new absorption bands in the red region. However for **3**, no new absorptions were observed. This can be explained as follows: the interaction of the phosphonate group with surface Ti ions is likely *via* formation of P—O—Ti bonds. Thus, the role of the PO_3H_2 is to serve as an interlocking group coupling electronically the π* orbitals of the terpy to the Ti 3d orbital manifold of the semiconductor similarly to COOH.[14] This coupling increases the delocalization of the π* orbitals of the terpyridine resulting in a decrease of the energy of the π* level and the red shift of absorption of **1** and **2** in the TiO_2 film. For **3**, the energy of the π* level of terpyridine is also lowered as for **1** and **2**, therefore, it might have been expected to show a redshifted absorption spectrum. However, it is known, for polypyridyl ruthenium(II) complexes, that the excited electron is localized on a single ligand, in complexes containing a mixed ligand set.[33] The excited electron is always localized on the ligand which is easier to reduce.[33] Biquin is more easily reduced than terpyridine, and the energy of the π* orbital of biquin is much lower than that of

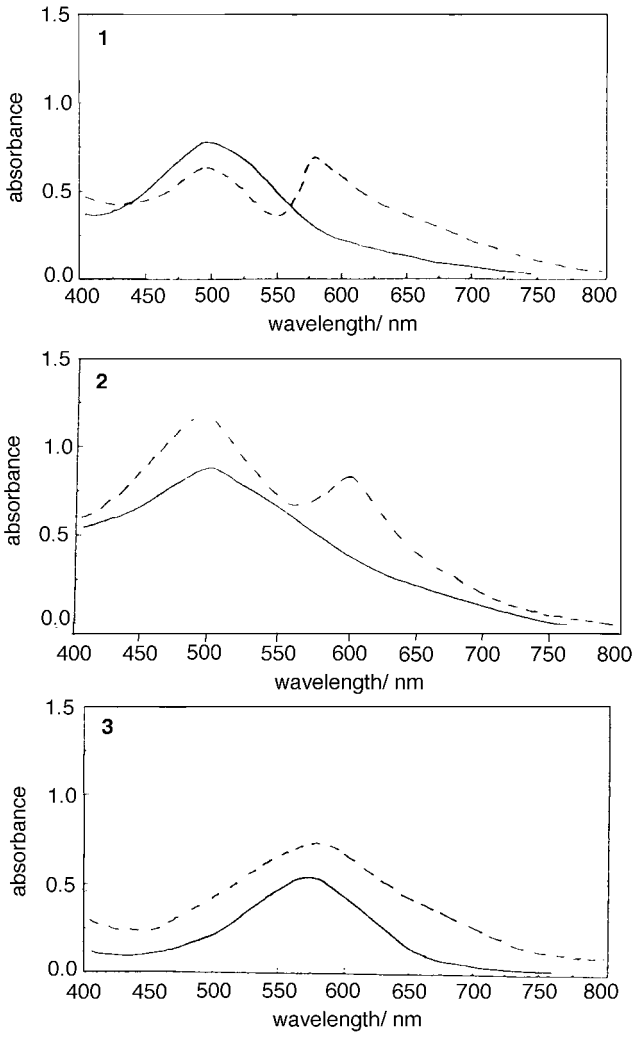

Fig. 2 Absorption spectra of complexes **1**, **2**, **3** on the TiO_2 film electrode, using a bare TiO_2 film electrode as a reference. — in film electrode, – – – in ethanol.

Table 1 Photophysical and electrochemical properties of complexes **1**–**3**

complex	λ_{abs}^{max}/nm[a] ($10^{-6}\varepsilon$/mol^{-1} cm^2)	$\lambda'_{abs}{}^{max}$/nm[b] pH 3	pH 9	λ_{em}^{max}/nm[a]	lifetime/ns	$10^5\phi$[c]	$E_{1/2}^{ox}$/V[d]
1	503(8.98)	490	506	735	41	6.7	0.86
2	497(9.92)	487	498	720	35	9.0	0.91
3	572(10.14)	561	581	~800[e]	—	—	1.00

[a]In ethanol. [b]In water. [c]In ethanol, measured relative to $[Ru(bpy)_3]^{2+}$ in aerated acetonitrile solution ($\phi = 0.012$), from *J. Am. Chem. Soc.*, 1982, **104**, 6620. [d]In DMF *vs.* SCE. [e]Very weak and broad at liquid N_2 temperature (77 K).

Table 2 Calculated LUMO energies of different ligands[a]

ligand	LUMO energy
dmpy	−0.50343
ttp	−0.67633
phen	−0.71796
biquin	−0.86120

[a]The two pyridine rings in dmpy and the three pyridine rings in ttp were constrained to be planar.

terpyridine (Table 2). The LUMO energies of ligands calculated by AM1 semi-quantitative quantum calculations reflect the ability of the ligands to accept an electron.

Owing to the large LUMO energy difference between biquin and ttp, even if the π* orbital energy (or LUMO) of the latter is somewhat decreased when attached onto TiO_2 electrode, this is not enough to alter the sequence of the π* orbital energy levels. Thus the excited electron is localized on biquin in complex **3** whether it is in solution or in TiO_2 film.The interaction of **3** with the TiO_2 surface does not involve the ligand relevant to MLCT, so the electronic spectrum of **3** adsorbed onto TiO_2 electrode does not show an observable change compared with its spectrum in solution. For **2**, while the LUMO energy of phen is slightly lower than that of ttp, the decrease of π* orbital energy (or LUMO) of ttp caused by the interaction with TiO_2 results in switching of their level order. When **2** is adsorbed onto TiO_2, the excited electron is now localized on ttp. The LUMO energy of dmpy in complex **1** is much higher than that of ttp so the excited electron is mainly localized on ttp both in solution and in the TiO_2 film. The interaction of either **1** or **2** with TiO_2 involves the MLCT ligand, so complexes **1** and **2** attached onto TiO_2 film electrodes exhibit electronic spectra different from their spectra in solution.

Photoelectrochemical properties

Fig. 3 shows a plot of incident-photo-to-current-efficiency, IPCE(λ), for three metal complexes anchored to TiO_2 electrodes. The measurements were made with an electrometer in a two-electrode arrangement and a 0.3 M LiI–0.03 M I_2 propylene carbonate electrolyte solution. The IPCE(%) is defined by eqn. (1):

$$\text{IPCE}(\%) = \frac{1.25\times10^3\ (\text{eV nm})\times\text{photocurrent density}\ (\mu\text{A cm}^{-2})}{\text{wavelength (nm)}\times\text{photoflux}\ (\mu\text{W cm}^{-2})} \quad (1)$$

Fig. 3 demonstrates that the IPCE is dependent on the surface attached compound. Maximum observed IPCE follows the trend: **1** > **2** ≫ **3** with complex **3** attached to TiO_2 film electrode showing virtually no photosensitization. The maximal IPCE of the TiO_2 film cell sensitized by **1** was >75% *cf.* 45% for **2**. The performances of the photoelectrochemical cells under white light illumination are is given in Table 3. Short circuit photocurrent densities, I_{sc}, and open circuit photovoltages V_{oc} were measured as described in the Experimental section. Current–voltage curves are shown in Fig. 4.

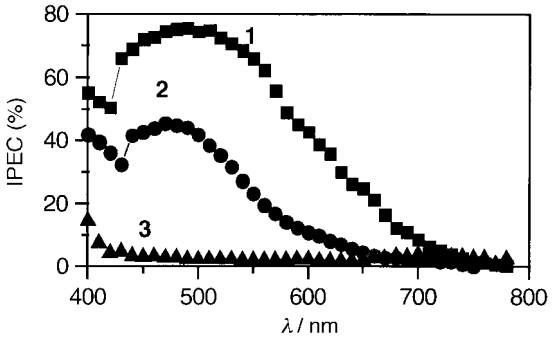

Fig. 3 Photoaction spectra of the sensitizers bound to TiO_2 in a regenerative solar cell

The fill factors were calculated from current–voltage curves. The best performance was shown by complex **1**. A key parameter of cell performance is the incident photon to current efficiency (IPCE), which directly reflects how efficiently incident photons lead to electrons. The IPCE is composed of three terms, expressed by eqn. (2):

$$\text{IPCE} = (\text{LHE})\phi\eta \quad (2)$$

where LHE is the light-harvesting efficiency, ϕ is the quantum yield for charge injection and η is the efficiency of collecting electrons on the external circuit, which reflects the probability that the injected electrons escape from recombination. In order to delineate the respective influences of the three factors on IPCE, it is necessary to compare the three parameters in eqn. (2).

Light harvesting efficiency

For a ideal sensitizer, all incident light power would be absorbed (LHE = 1), but this is actually never observed. The absorption factor (α) is the product of the radiant power absorbed by the system, I, divided by the incident radiant power, I_0, $\alpha = I/I_0$.[34] In photoelectrochemical literature, the absorption coefficient is expressed as the LHE. If losses are caused only by transmission of light, $\text{LHE} = \alpha = I/I_0 = 1 - T = 1 - 10^{-A}$, where T is the transmittance and A is the absorbance.[34] Assuming Beer's law is applicable, LHE (λ) can be related to the molar absorption coefficient by eqn. (3):

$$\text{LHE}(\lambda) = 1 - 10^{-\varepsilon\Gamma} \quad (3)$$

where Γ is the surface coverage (mol cm^{-2}) and ε is the dye's molar absorption coefficient (mol^{-1} cm^2) at wavelength λ. LHE at the MLCT maximum and the measured surface coverages are given in Table 3. The coverages of complexes **1**–**3** attached to the surface of electrodes and molar absorption coefficients given in Table 1 and Table 3 only show small changes. Thus, LHE is not the main reason that leads to the large differences in IPCE. It is worthwhile to point out that the values of LHE reported here are lower limits, if scattering is taken into account. The LHE calculated according to Beer's law is only strictly correct for transparent TiO_2 films. The films prepared from Degussa P25 particles scatter light. Hence,

Table 3 Photoelectrochemical properties of complex attached to TiO_2 film electrodes

complex	max. IPCE(%)[a]	I_{sc}[b]/mA cm^{-2}	V_{oc}[b]/mV	ff[b]	$10^7\Gamma$[c]/mol cm^{-2}	LHE(%)[d]
1	75.6	4.73	0.653	0.705	1.37	94.1
2	45.4	1.88	0.625	0.814	1.42	96.1
3	1.74	0.368	0.445	0.750	1.10	92.3

[a]Maximum incident photon to current conversion efficiency from Fig. 3. [b]Short circuit photocurrent (I_{sc}), open circuit photovoltage (V_{oc}) and fill factor(ff) obtained in a sandwich cell arrangement with white light excitation (Fig. 4). [c]Surface coverage of complex. [d]Light harvesting efficiency at wavelength of maximum absorption.

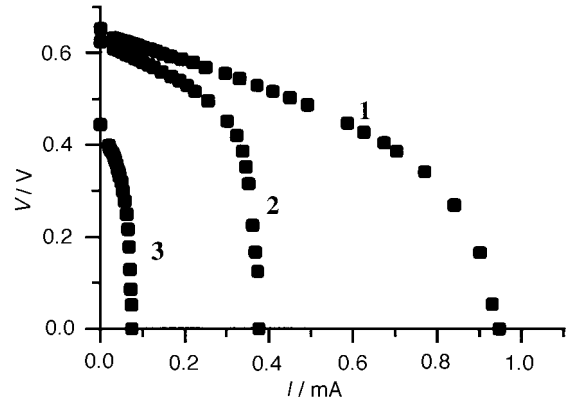

Fig. 4 Photocurrent-curves of the photoanodes in a regenerative dye-sensitized solar cell under white light excitation. 0.2 cm^2 active area was radiated.

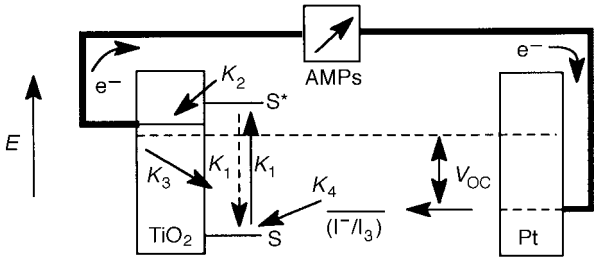

Fig. 5 An accepted model for dye sensitization in regenerative photoelectrochemical cells

their LHE is higher than that of transparent films as the optical path length is increased by the scattering.

Electron collection efficiency

A remarkable property of TiO_2 nanocrystalline films is their ability to efficiently collect electrons through a thick porous colloidal semiconducting layer. Resistive losses within the nanostructured TiO_2 film are expected to be independent of the surface attached dye. Fig. 5 illustrates a generally accepted model for dye sensitization of wide-bandgap semiconductors.[35] The recombination rate of injected electrons with the oxidized dye (k_3) is an important factor affecting electron collection efficiency (η), which will decrease with increasing k_3.

For complexes **1**–**3**, the recombination of the injected electrons with the oxidized dyes, if anything, should be more efficient for **1** due to the higher surface concentration of oxidized donors produced by the larger photocurrent density. Marcus has shown that, under a high-temperature approximation, the non-adiabatic electron-transfer rate between two electronic levels can be expressed by eqn. (4):

$$k_{et} = \frac{2\pi|H_{DA}|^2}{h(4\pi\lambda RT)^{1/2}} \exp\frac{-(\Delta G^0+\lambda)^2}{4\lambda RT} \quad (4)$$

where H_{DA} is the electronic coupling matrix element, ΔG^0 is the free energy change for electron transfer process, and λ is the free energy of reorganization. We can estimate ΔG^0 for electron transfer from the conduction band edge to the oxidized dyes as $\Delta G_1{}^0 = -1.26$ eV for complex **1**, $\Delta G_2{}^0 = -1.31$ eV for complex **2**, $\Delta G_3{}^0 = -1.40$ eV for complex **3** (here $E_{CB} = -0.4$ V is assumed[21]). Reorganizational energies for the three complexes in this study are expected to be similar, and a typical value in related polypyridyl ruthenium complexes is 0.5 eV.[36] These electron transfer processes should fall in the inverted region when $-\Delta G^0 > \lambda$. The larger the value of ΔG^0, the lower the electron transfer rate. So, the rates of the electron transfer from the conduction band to the oxidized dyes, k_3, for complexes **1**–**3** should be $k_{31} > k_{32} > k_{33}$ where k_{31}, k_{32} and k_{33} represent the rate of electron transfer of complexes **1**, **2** and **3** respectively. Therefore, the molecular level similarity of the dyes and the relative values of k_3 allow us to conclude that η is not the cause of the differences in IPCE.

Electron injection quantum yield

Electron transfer from the excited dye to the TiO_2 surface will be an activationless process, if there is maximum overlap between the excited donor levels and the wide conduction band acceptor. The rate of activationless electron transfer from dye molecules to semiconductor surfaces is ultrafast and a lower limit of $k_2 > 10^9$ s^{-1} has been recently measured.[37] The quantum yield for electron injection (ϕ) is given by eqn. (5):

$$\phi = k_2/(k_2 + k_r + k_{nr}) \quad (5)$$

where k_r and k_{nr} are the radiative and non-radiative rate constants for the excited dye and k_2 is the electron injection rate (Fig. 5). A lower ϕ would occur if radiative or non-radiative decay competes with electron injection. If the electron injection process is activated, the electron transfer rate will also decrease. As an approximation, electrochemical and spectroscopic data obtained in fluid solution can be used. The flat potential of TiO_2 film electrodes is -0.55 V (SCE) obtained from a Mott–Schottky curve which was determined by using a three-electrode system in MeCN. We employ the Rehm–

Table 4 Photophysical and electrochemical properties of **1**–**3** and the free energy changes of the electron transfer from the excited states of complex **1**–**3** to TiO_2 film electrodes

complex	E_{ox} (D)[a]/V	E_{red} (A)[b]/V	$\lambda_{abs}{}^{max}$/nm[c]	$\lambda_{em}{}^{max}$/nm	E^{0-0}/eV[d]	ΔG^0/eV
1	0.86		503	735[c]	2.003	−0.653
2	0.91	−0.55	497	710[c]	2.054	−0.654
3	1.00		572	~800[e]	1.807	−0.317

[a]In DMF. [b]In CH_3CN. [c]In ethanol. [d]$E^{0-0} = (\lambda_{abs}{}^{max} + \lambda_{em}{}^{max})/2$ as an approximation. [e]Very weak and broad under liquid nitrogen.

Weller equation [eqn. (6)]

$$\Delta G^0 = E_{ox}\,(D) - E_{red}\,(A) - E^{0-0} - C \qquad (6)$$

where ΔG^0 is the free energy change of the electron transfer from the excited dye to the TiO_2 conduction band, $E_{ox}(D)$ is the ground oxidation potential of the dye, $E_{red}(A)$ is the flat potential of TiO_2, E^{0-0} is the zero–zero excitation energy and C is *ca.* 0.06 in MeCN. According to the Rehm–Weller equation, the free energy of electron transfer from the excited dye to the conduction band of TiO_2 is <0 (Table 4), so the electron injection processes are activationless for all the sensitizers. Therefore, an activated electron transfer process cannot explain the large differences of complexes **1**–**3** in IPCE.

As is well known for transition metal complexes, only the lowest excited state has a chance to emit luminescence and /or to live long enough to participate in bimolecular process. In the great majority of ruthenium(II) polypyridine complexes, the lowest excited state is a ^{3}MLCT level (*i.e.*, metal-to-ligand change transfer). Extensive investigation of ruthenium polypyridine complexes have given evidence for a single ligand localized excited state on the timescale of molecular vibrations with the excited electron localized on the ligand which is easier to reduce.[33] As mentioned above, for complexes **1**, **2** and **3**, the excited electron is mainly localized on ttp-PO_3H, phen and biquin, respectively in solution. When attached to the TiO_2 electrode, the excited electrons are still localized on biquin in complex **3** and on ttp-PO_3H in complex **1** because of the large π^* orbital energy differences between ttp-PO_3H *cf.* biquin and dmpy. The excited electron can be partly localized on ttp-PO_3H or phen in complex **2** because of the small π^* orbital energy differences between ttp-PO_3H and phen. Within the timescale of molecular vibrations, if the excited electron is not transferred in time to the TiO_2 conduction band, it will be deactivated undergoing radiative or non-radiative processes. Because the excited electron of complex **1** is localized on the ligand ttp-PO_3H attached to the TiO_2 electrode, it can be injected efficiently into the TiO_2 conduction bands leading to the best IPCE. For complex **2**, lower IPCE is shown because only some of the excited electrons are localized on ttp-PO_3H. The excited electron of complex **3** is localized on biquin which is remote from the TiO_2 electrode, and its excited state deactivates mainly by the way of non-radiation and hence **3** exhibits the lowest sensitization to the TiO_2 electrode.

Conclusion

The differences exhibited in photo-electricity conversion for complexes **1**, **2** and **3** are mainly related to the competition of the excited state deactivation through radiative or non-radiative processes with electron injection to TiO_2. In other words, different electron injection efficiencies originating from the localization of the excited electron lead to differences in IPCE of complexes **1**, **2** and **3**. Therefore, for high efficiency, the adsorbent groups should be localized on the ligand whose lowest unoccupied molecular orbital energy is lowest in the complex, making the excited electron localize on this ligand and efficiently injecting into the conduction band of the semiconductor. This work also demonstrates the localization of the excited electron in ruthenium polypyridine complexes from sensitization of Ru to TiO_2 electrodes.

References

1 M. A. Fox and M. Chanon *Photoinduced Electron Transfer*, Elsevier, Amsterdam, 1988.
2 M. Gratzel, *Heterogeneous Photochemical Electron Transfer*, CRC Press, Boca Raton, FL, 1989.
3 *Photosensitization and Photocatalysis Using Inorganic and Organometallic Compounds*, ed. K. Kalyanasundaram and M. Gratzel, Kluwer Academic Publishers, Dordrecht, 1993, p. 248.
4 S. R. Morrison, *Electrochemistry of Semiconductor and Oxidized Metal Electrodes*, Plenum Press, New York, 1980 and references therein.
5 W. A. Nevin and G. A. Chamberlain, *J. Appl. Phys*., 1991, **69**, 4324.
6 G. D. Sharma, S. C. Mathup and D. C. Dube, *J. Mater. Sci*., 1991, **26**, 6547.
7 H. Gerischer in *Photoelectrochemistry, Photocatalysis and Photoreaction*, ed. M. Schiavello, D. Reidel, Dordrecht, 1985.
8 B. O'Regan and M. Gratzel, *Nature (London)*, 1991, **353**, 737.
9 J. Desilvestro, M. Gratzel, L.Kavan, J. Moser and J. Augustynski, *J. Am. Chem. Soc*., 1985, **107**, 2988.
10 K. Kalyanasundaram, N. Vlachopoulos, V. Kishnan, A. Monnier and M. Gratzel, *J. Phys. Chem*., 1987, **91**, 2342.
11 N. Vlachopoulos, P. Liska, J. Augustynski and M. Gratzel, *J. Am. Chem. Soc*., 1988, **110**, 1216.
12 P. Liska, N.Vlachopoulos, M. K. Nazeeruddin and M. Gratzel, *J. Am. Chem. Soc*., 1988, **110**, 3686.
13 O. Enea, J. Moser and M. Gratzel, *J. Electroanal. Chem*., 1989, **259**, 59.
14 M. K. Nazeeruddin, P. Liska, J. Moser, N. Vlachopoulos and M. Gratzel, *Helv. Chim. Acta*., 1990, **73**, 1788.
15 M. K. Nazeeruddin, A. Kay, I. Rodicio, R. Humphry-Baker, E. Muller, P. Liska, N. Vlachopoulos and M. Gratzel, *J. Am. Chem. Soc*., 1993, **115**, 6382.
16 A. Kay and M. Gratzel, *J. Phys. Chem*., 1993, **97**, 6272.
17 P. Pechy, F. P. Rotzinger, M. K. Nazeeruddin, O. Kohle, M. Zakeeruddins, R. Humphry-Baker and M. Gratzel, *J. Chem. Soc., Chem. Commun*., 1995, **1**, 65.
18 O. Kohle, S. Ruike and M. Gratzel, *Inorg. Chem*., 1996, **35**, 4779.
19 R. Dabestani, A. J. Bard, A. Campion, A. Campion, M. A. Fox, T. E. Mallouk, S. E. Webber and J. M. White, *J. Phys. Chem*., 1988, **92**, 1872.
20 R. Amadelli, R. Argazzi, C. A. Bignozzi and F. Scadola, *J. Am. Chem. Soc*., 1990, **112**, 7099.
21 T. A. Heimer, C. A. Bignozzi and G. J.Meyer, *J. Phys. Chem*., 1993, **97**, 11 987.
22 G. Smestad, C. A. Bignozzi and R. Argazzi, *Sol. Energy Mater. Sol. Cells*, 1994, 32, 259.
23 R. Argazzi, C. A. Bigozzi, T.A. Hemer, F. N. Gastellano and G. J. Meyer, *Inorg. Chem*., 1994, **33**, 5741.
24 C. A. Bignozzi, R. Argazzi, J. R. Schoonover, G. J. Meyer and F. Scandola, *Sol. Energy Mater. Sol. Cells*, 1995, **38**, 187.
25 V. Balzai, S. Campagna, G. Denti, A. Juris, S. Serroni and M. Venturi, *Sol. Energy Sol. Cells*, 1995, **38**, 159.
26 R. Argazzi, C. A. Bignozzi, T. A. Heimer, F. N. Castellano and G. J. Meyer, *J. Am.Chem. Soc*., 1995, **117**, 11 815.
27 Weibo Wang, Zhenzhong Zhang and Xuri Xiao, *Chin. Sci. Bull*., 1996, **41**, 1468.
28 Cheng Lifang, Wang Yu and Dai Songyuan., *Chin. Mater. Res*., 1996, **10**, 404.
29 T. A. Heimer, S. T. D'Arcangelis, F. Farzad, J. M. Stipkala and G. J. Meyer, *Inorg. Chem*., 1996, **35**, 5319.
30 I. Bedja, S. Hotchandani and P. V. Kamat, *J. Phys. Chem*., 1994, **98**, 4133.
31 P. V. Kamat, I. Bedja, S. Hotchandani and L. K Patterson, *J. Phys. Chem*., 1996, **100**, 4900.
32 H. Toshikazu, M. Toshio, O. Yoshiki and A. Toshio, *Synthesis*, 1981, 56.
33 A. Junis, V. Balzani, F. Barigelletti, S. Campagna, P. Belser and A. Von Zelewsky, *Coord. Chem. Rev*., 1988, **84**, 139.
34 N. Sheppard, H. Willis and J. C. Rigg, *Pure Appl. Chem*., 1985, **57**, 105.
35 G. J. Meyer, *J. Chem. Educ*., 1997, **74**, 652.
36 S. R. Lunt, L. G. Gasagrande, B. J. Tufts and N. S. Lewis, *J. Phys. Chem*., 1988, **92**, 5766.
37 (*a*) R. Eichberger and F. Willig, *Chem. Phys*., 1990, **141**, 159; (*b*) F. Willig, R. Eichberger, N. S. Sundaresan and B. Parkinson, *J. Am. Chem. Soc*., 1990, **112**, 2702.

Paper 8/02489H; *Received* 26*th February*, 1998